

# Energy efficiency of neptunium redox battery in comparison with vanadium battery

T. Yamamura, N. Watanabe, Y. Shiokawa\*

*Institute for Materials Research, Tohoku University, 2-1-1 Katahira, Sendai, Miyagi 980-8577, Japan*

Available online 28 June 2005

## Abstract

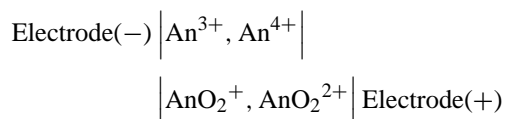
A neptunium ion possesses two isostructural and reversible redox couples ( $\text{Np}^{3+}/\text{Np}^{4+}$  and  $\text{NpO}_2^+/\text{NpO}_2^{2+}$ ) and is therefore suitable as an active material for a redox-flow battery. Since the plastic formed carbon (PFC) is known to show the largest  $k_0$  values for  $\text{Np}(\text{IV})/\text{Np}(\text{III})$  and  $\text{Np}(\text{V})/\text{Np}(\text{VI})$  reactions among various carbon electrodes, a cell was constructed by using the PFC, with the circulation induced by bubbling gas through the electrolyte. In discharge experiments with a neptunium and a vanadium battery using the cell, the former showed a lower voltage loss which suggests a smaller reaction overvoltage. Because of the high radioactivity of the neptunium, it was difficult to obtain sufficient circulation required for the redox-flow battery, therefore a model for evaluating the energy efficiency of the redox-flow battery was developed. By using the known  $k_0$  values for neptunium and vanadium electrode reactions at PFC electrodes, the energy efficiency of the neptunium battery was calculated to be 99.1% at  $70 \text{ mA cm}^{-2}$ , which exceeds that of the vanadium battery by ca. 16%.

© 2005 Elsevier B.V. All rights reserved.

**Keywords:** Redox-flow battery; Neptunium battery; Vanadium battery; Energy efficiency

## 1. Introduction

Neptunium has two isostructural couples,  $\text{Np}^{n+}$  ( $n = 3$  and  $4$ ) and  $\text{NpO}_2^{(n-4)+}$  ( $n = 5$  and  $6$ ), in acidic solutions, where  $n$  is the oxidation state of the neptunium. This structural feature that the neptunium has two isostructural couples is a unique chemical nature of the light actinide and it accompanies the fast electron transfer reactions in each couple. In addition, the redox potentials of these neptunium couples are as far apart as possible within the potential window of the acidic water;  $E^0 = 0.15 \text{ V}$  for  $\text{Np}^{3+}/\text{Np}^{4+}$  and  $E^0 = 1.14 \text{ V}$  for  $\text{NpO}_2^+/\text{NpO}_2^{2+}$  in  $1 \text{ M HCl}$  [1]. These distinctive electrochemical properties of the aqueous solutions of  $\text{Np}^{3+}/\text{Np}^{4+}$  and  $\text{NpO}_2^+/\text{NpO}_2^{2+}$  are in accordance with what is desired for electrolytes in a redox-flow battery. Thus, an all-neptunium redox-flow battery is proposed as follows:



where An is neptunium [2]. The all-neptunium battery uses only a single element, so that it can avoid the progressive deterioration of the positive- and negative-electrolytes due to the mutual contamination of the electrolytes through an ion exchange membrane, as observed for the Fe–Cr battery [3] that uses two elements.

An all-uranium redox-flow battery has been proposed and investigated by Shiokawa and co-workers [2,4–6]. The importance of a uranium redox-flow battery lies in the potential utilization of the huge amount of stored depleted uranium produced in the nuclear power industry. The uranium battery requires aprotic organic systems excluding the proton cation which promotes the disproportionation reaction of  $\text{UO}_2^+$  to  $\text{U}^{4+}$  and  $\text{UO}_2^{2+}$  [7–16]. In contrast, the four neptunium ions ( $\text{Np}^{3+}/\text{Np}^{4+}$  and  $\text{NpO}_2^+/\text{NpO}_2^{2+}$ ) are stable in aqueous solutions and the neptunium battery is suitable for fundamental investigations of actinide batteries, including the all-uranium battery.

The existing all-vanadium battery with carbon felt electrodes [17] has relatively high energy efficiencies of 87.8%, 86% and 80.6% at  $25 \text{ mA cm}^{-2}$ ,  $40 \text{ mA cm}^{-2}$  and  $60 \text{ mA cm}^{-2}$ , respectively [18], when the area of the carbon felt sheet is evaluated like the surface area of the plate.

\* Corresponding author. Fax: +81 22 215 2121.

E-mail address: shiokawa@imr.tohoku.ac.jp (Y. Shiokawa).

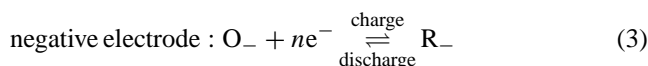
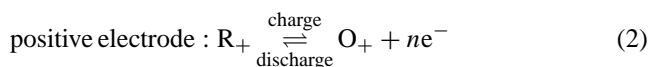
But the effective current densities based on the effective surface areas of carbon fibers comprising the carbon felt electrode are much smaller. A low current density is required when the reaction overvoltage is high, owing to small standard rate constants of the redox reactions of  $V^{2+}/V^{3+}$  and  $VO^{2+}/VO_2^+$  of  $k_0 = 1.75 \times 10^{-5} \text{ cm s}^{-1}$  and  $7.5 \times 10^{-4} \text{ cm s}^{-1}$ , respectively [19,20]. Although the slow kinetics of  $VO^{2+}/VO_2^+$  is attributed to the oxygen-involving redox reaction, the reason for the slow kinetics of  $V^{2+}/V^{3+}$  has not been clearly elucidated or understood [21,22].

Energy efficiency of the redox-flow battery should be governed by various electrochemical factors including (i) resistive losses in the electrolytes, membrane and electrodes, (ii) mass transfer losses in the electrolyte, (iii) loss of faradic efficiency due to crossover of ions through the membrane, (iv) loss of faradic efficiency due to possible side reactions and (v) loss of voltage efficiency due to large overvoltage for electrode reactions with slow kinetics. Although an estimation of the energy efficiency of redox-flow battery should be quite difficult, provided that those factors from (i) to (iv) are common to certain two types of batteries with different active materials, comparison of the energy efficiency is possible by estimating kinetic factors, i.e. the factor (v). Since the redox-flow battery of neptunium and that of vanadium have similar aqueous solution, i.e. nitric acidic solution and sulfuric acidic solution, respectively, a comparison of the energy efficiency of these two types of the redox-flow batteries can be performed on the basis of the overvoltage caused by the kinetic parameters of neptunium and vanadium electrode reactions. Recently, we reported standard rate constants at the plastic formed carbon (PFC) electrode for  $Np(IV)/Np(III)$  ( $k_0 = 1.4 \times 10^{-2} \text{ cm s}^{-1}$ ) and  $Np(V)/Np(VI)$  ( $k_0 = 2.1 \times 10^{-2} \text{ cm s}^{-1}$ ) [23].

In the present study, the discharge performance of a neptunium battery equipped with a carbon electrode has been investigated and compared with the performance of the existing vanadium battery. The electrode material with the largest  $k_0$  value was selected and the discharge curves were obtained for the neptunium battery. Discharge curves were also obtained for the vanadium battery in an identical small cell. Because of the difficulty in achieving sufficient circulation of the highly radioactive neptunium solution in the battery by pumping, it would not be enough to demonstrate the energy efficiency of the neptunium battery due to the concentration polarization which can result in the overvoltage. Therefore, we also investigated the neptunium battery in general to demonstrate its performance. The overvoltage of the electrode reaction, and thus the voltage efficiency, equivalent to the energy efficiency when the coulombic efficiency is unity, was evaluated because the battery reaction is a typical heterogeneous reaction through the electrode-liquid interface. Thus, the formulation of energy efficiency for the redox-flow battery with a given active material was determined, and applied to both the neptunium and the vanadium batteries.

## 2. Formalism of energy efficiency of redox-flow batteries

The redox-flow battery does not involve any deposition process during the charge–discharge cycles, but incorporates typical electron transfer heterogeneous processes on the electrodes. Therefore, the overvoltage in these heterogeneous processes should be treated by the typical current–overpotential relationship under rigorous stirring, i.e. the Butler–Volmer equation [24]. We can consider the charge–discharge process of the redox-flow batteries composed of two redox pairs of the positive electrolyte ( $O_+/R_+$ ) and that of the negative electrolyte ( $O_-/R_-$ ). In the discharge process, the electron produced in the oxidation reaction in the negative electrolyte is supplied to the negative electrolyte, wherein the electron is consumed in the reduction reaction. These two parallel redox reactions are as shown below



The Nernst potentials of the positive and negative electrolytes,  $E_+$  V and  $E_-$  V, are given by

$$E_{\pm} = E_{\pm}^0 - \frac{RT}{nF} \ln \left[ \frac{O_{\pm}}{R_{\pm}} \right] \quad (4)$$

where  $E_+^0$  and  $E_-^0$  designate the standard electrode potentials of the redox couples of  $O_+/R_+$  and  $O_-/R_-$ , respectively. The difference  $E_{\text{open}} = (E_+ - E_-)$  V corresponds to the open circuit voltage of the battery. Under a current density larger than zero, the battery voltage differs from  $E_{\text{open}}$  according to the relationship between the current density and the activation overpotential, i.e. the Butler–Volmer equation as,

$$j_{\pm} = j_{0,\pm} \{ \exp(-\alpha n f \eta_{\pm}) - \exp((1 - \alpha) n f \eta_{\pm}) \} \quad (5)$$

where  $\eta$  V is the overvoltage. The current density,  $j$  A  $\text{cm}^{-2}$ , is defined to be positive when the electron is consumed at the electrodes by the reduction reaction. The ‘+’ and ‘-’ subscripts indicate the positive and the negative electrodes, respectively. The exchange current density  $j_0$  is a function of the concentrations of the oxidized and the reduced form ( $C_{\text{ox}}$  and  $C_{\text{red}}$ , respectively) and the standard rate constants of the positive  $k_{0,p}$  and the negative  $k_{0,n}$  electrodes. The charged energy  $E_c$  and the discharged energy  $E_d$  are obtained by integrating the operating voltages of the charging process  $V_c$  V and the discharging process  $V_d$  V at the current density  $j$  by the charged or discharged electric charge  $Q_c$  C and  $Q_d$  C as

$$\begin{aligned} E_c &= \int_0^{Q_c} V_c dQ \\ &= E_{\text{open}} Q_c + \int_0^{Q_c} (\eta_+ - \eta_-) dQ + R \int_0^{Q_c} j_c dQ \quad (6) \end{aligned}$$

$$E_d = \int_0^{Q_d} V_d dQ$$

$$= E_{\text{open}} Q_d + \int_0^{Q_d} (\eta_+ - \eta_-) dQ - R \int_0^{Q_d} j_c dQ \quad (7)$$

where  $E_{\text{open}} = \eta_+ - \eta_-$  and  $R \Omega \text{ cm}^2$  designates the inner electrical resistance of the battery. On the right-hand side of the above two equations, the first, the second and the third terms correspond to the energy required to charge or discharge the battery reversibly, the energy required against the overvoltage dissipated as the heat, and the energy consumed due to the internal resistance, respectively. The value of  $E_d/E_c$  for a cycle with  $Q_c$  and  $Q_d$  corresponds to the energy efficiency. In the present study, by assuming that the Coulombic efficiency  $Q_d/Q_c$  is unity, the energy efficiency, equivalent to the voltage efficiency, is to be evaluated.

### 3. Experimental

#### 3.1. Discharge experiments of neptunium and vanadium batteries

The cell used in the discharge experiments was equipped with an ion exchange membrane, which divides the cell into two compartments each with a volume of 18 mL. The ion exchange membranes used for the vanadium and the neptunium solutions were K-501 and A-511, the cation and the anion exchange membranes, respectively, both being products of Asahi Kasei Corp., Japan. Within each compartment, a single plate of an electrode was installed, whose 4 cm<sup>2</sup> surface area made contact with each electrolyte. The distance between the electrodes was 34 mm. The stirring of the electrolyte solutions was carried out using bubbling argon gas in order to avoid the experimental difficulties associated with the circulation of highly radioactive neptunium by pumping.

A neptunium-237 solution, possessed by the Institute for Materials Research, Tohoku University, was purified before use by the lanthanum fluoride co-precipitation method for the recovery of purified neptunium, as already described [23]. For preparing the charged state of the neptunium battery, an 8 mL portion of 1 mol dm<sup>-3</sup> nitric acidic solution of 0.05 mol dm<sup>-3</sup> neptunium was poured into each compartment in the cell. These were electrolyzed at a constant current of 5 mA using a galvanostat (HA-501, Hokuto Denko Co. Ltd., Japan) at the gold electrodes to obtain Np(VI) and Np(III) for the positive and the negative electrolytes, respectively. In the case of the vanadium battery, an 8 mL portion of 1 mol dm<sup>-3</sup> sulfuric acidic solution of 0.05 mol dm<sup>-3</sup> VOSO<sub>4</sub> was used as the positive electrolyte. For the negative electrolyte, this solution was first reduced under a constant voltage to obtain 8 mL of V(III) solution. For the discharge experiments, plastic formed carbon (PFC) was used for the electrode because the PFC yields the largest standard rate constants for both Np(V)/Np(VI) and Np(IV)/Np(III) reactions, as will be

Table 1

Specifications of the redox-flow battery assumed for the energy efficiency evaluation

Equilibrium electrode potential of the positive electrode (V)	1.00
Equilibrium electrode potential of the negative electrode (V)	-0.30
Concentration of active materials in both cells (mol dm <sup>-3</sup> )	1.0
Transfer coefficients of both electrodes	0.5
Internal resistance of the battery ( $\Omega \text{ cm}^2$ )	0
Surface area of the electrode (cm <sup>2</sup> )	1
Volume of the electrolyte solutions (cm <sup>3</sup> )	10

described later. For the measurement of the discharge curves, an appropriate electrical resistor as a resistance load was connected between the positive and the negative electrodes of the cell. The voltage between the two ends of the load resistor was monitored and recorded every 1 s using a voltage recorder (NR-1000, Keyence Corporation, Japan) connected to a computer.

#### 3.2. Calculation of charge and discharge curves, and energy efficiency of the batteries

The redox-flow batteries assumed in the energy efficiency evaluation are composed of two redox pairs, R<sub>+</sub>/O<sub>+</sub> and R<sub>-</sub>/O<sub>-</sub>, as shown in reactions (2) and (3). Other specifications for the batteries are shown in Table 1. Charged condition of the battery is defined as that 99.5% of active material is oxidized form (O<sub>+</sub>) in the positive electrolyte and 0.5% is oxidized form (O<sub>-</sub>) in the negative electrolyte. Discharged condition is just reversely defined as 0.5% of active material is oxidized form (O<sub>+</sub>) in the positive electrolyte and 99.5% is oxidized form (O<sub>-</sub>) in the negative electrolyte. Based on the above conditions, the charged and the discharged energy was estimated to be 1242 J. The charge–discharge model computer program, described in the theory section, was written in the Pascal language (Delphi, Borland Software Corp., USA) and was run on a PC. The calculations of the charge transfer between the electrolytes were performed at every 0.01 C change. The calculations of the charge and discharge curves are performed at specific  $k_0$  values, for which the values of the standard rate constants of the positive  $k_{0,p}$  and the negative  $k_{0,n}$  electrodes are identical to  $k_0$ .

### 4. Results and discussion

#### 4.1. Demonstration of neptunium battery

The discharge curves of the vanadium battery were obtained by using the cell constructed in the present study filled with an electrolyte of 1 mol dm<sup>-3</sup> sulfuric acid with 0.05 mol dm<sup>-3</sup> vanadium. The discharge curves obtained by connecting 10 M $\Omega$ , 5 k $\Omega$  and 500  $\Omega$  resistors are shown in Fig. 1(b). When the 10 M $\Omega$  or 5 k $\Omega$  resistors were used, the voltages plateaued after the initial 15–30 min owing to very small currents, less than a milliampere in these cases. The plateau values for 10 M $\Omega$  and 5 k $\Omega$  were ca. 1.3 V and 1.2 V,

respectively, which are close to the open circuit voltage of the vanadium battery with a full charge. Therefore, these plateaus indicate open circuit voltage. During the charging process, corrosion of the positive PFC electrode was observed and small black particles, probably made of carbon, were found suspended in the positive electrolyte. Owing to this phenomenon, only the discharge curves of the batteries were obtained and compared.

The electrolyte of the neptunium battery was  $1 \text{ mol dm}^{-3}$  nitric acid with  $0.05 \text{ mol dm}^{-3}$  neptunium. Initially, both compartments were filled with Np(V) and Np(VI) mixed solution, and electrolysis at a constant current was carried out to produce the charged state, i.e. Np(III) and Np(VI). In the charging process, gold electrodes ( $30 \text{ mm} \times 8 \text{ mm}$ ) were used because the charging by the PFC electrodes resulted in the corrosion in both the positive and negative electrodes. After charging, the discharge curves were obtained, as shown in Fig. 1(a), using the PFC electrodes and by connecting a  $10 \text{ k}\Omega$  or  $500 \Omega$  resistor. When the  $10 \text{ k}\Omega$  resistor was used, the voltage became nearly constant, after the initial decrease, within 10 min. Thus, the  $10 \text{ k}\Omega$  resistor was used to obtain the open circuit voltage of ca. 1.1 V.

As seen in the Fig. 1, the battery voltage shows a large reduction when compared with the open circuit voltage in both batteries. This reduction may originate from the inner resistance, which could be larger than the load resistance owing to insufficient stirring and the relatively small concentration of the electrolytes. As mentioned earlier in the

Section 2, the stirring of the electrolytes was performed by the bubbling of argon gas. The gas flow was limited to a gas bubble per second in order to prevent the electrolytes from spilling out. This level of stirring was insufficient and the inner resistance likely became large owing to a large concentration polarization. Moreover, the small concentration of the active materials in the present study leads to the small exchange current density which then results in the small current density according to Eq. (5). This reduction in the current density has an equal effect with the large inner resistance appeared in Eqs. (6) and (7). Thus, the circulation by pumping is desired for the forthcoming charge–discharge experiments of the uranium battery which is not the highly-radioactive material unlike the neptunium.

Fig. 2 shows photographs of the neptunium battery in a charged state (upper photo) with Np(VI) and Np(III) in the

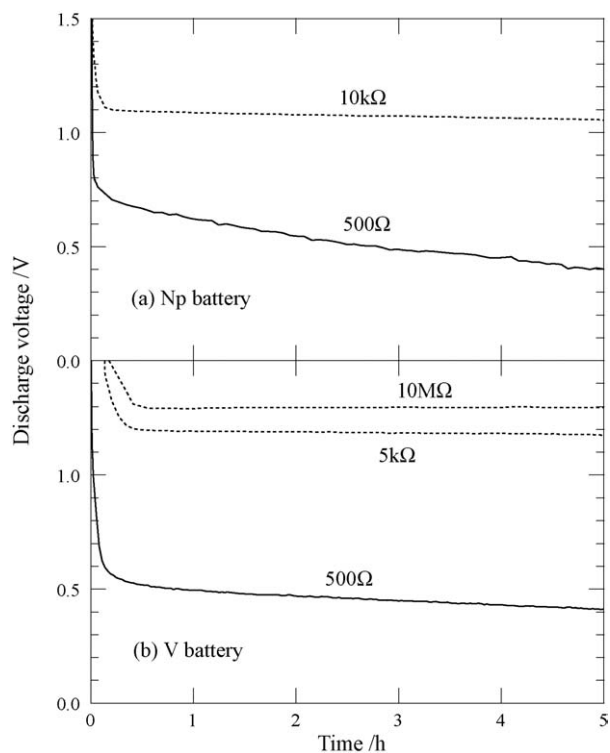


Fig. 1. Discharge curves of  $0.05 \text{ mol dm}^{-3}$  neptunium battery with  $1 \text{ mol dm}^{-3}$   $\text{HNO}_3$  (a) and  $0.05 \text{ mol dm}^{-3}$  vanadium battery with  $2 \text{ mol dm}^{-3}$   $\text{H}_2\text{SO}_4$  (b).

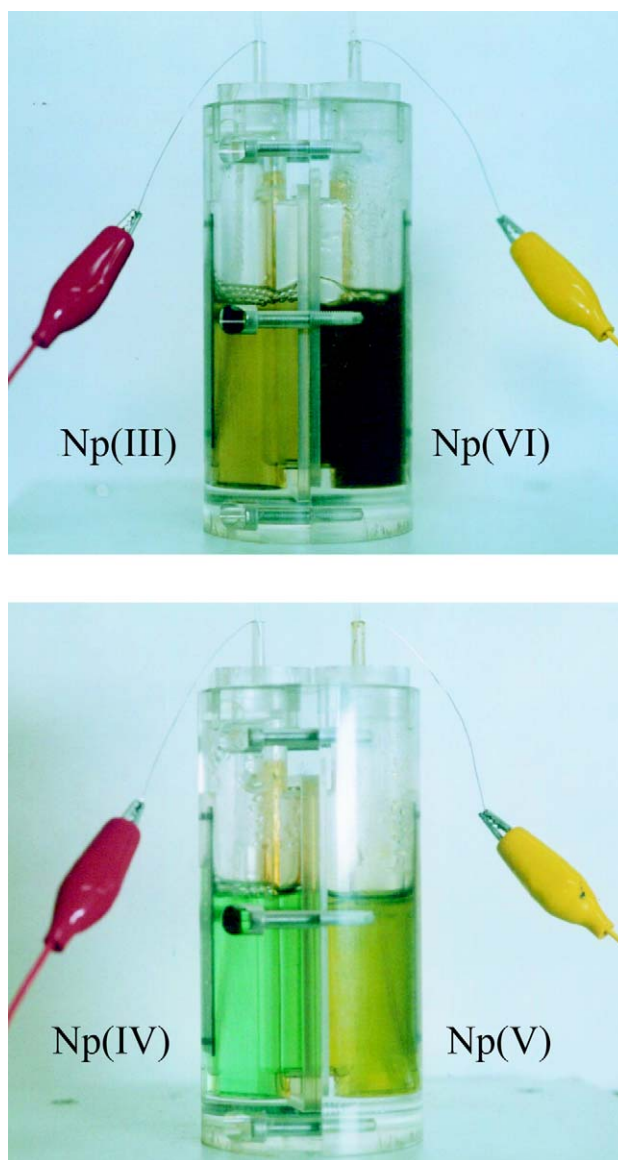


Fig. 2. Photographs of charged (upper picture) and discharged (lower picture) neptunium battery.

positive and the negative electrolytes, respectively, and in a discharged state (lower photo) with Np(V) and Np(IV) in the positive and the negative electrolytes, respectively. The solution colors were light brown, light green, yellow-green and dark brown for Np(III), Np(IV), Np(V) and Np(VI) solutions, respectively. These colors are somewhat different from the colors reported in literature which were green to blue, yellow-green, green and pink to red for Np(III), Np(IV), Np(V) and Np(VI) solutions, respectively [25]. This discrepancy is presumably due to the formation of charge transfer band in the presence of the nitric acid in the present study.

#### 4.2. Dependence of energy efficiency on standard rate constants of active materials

Fig. 3 shows the results of the calculated charge and discharge curves at a constant current density of  $70 \text{ mA cm}^{-2}$  for various  $k_0$  values. In the case of  $k_0 = 10^{-1} \text{ cm s}^{-1}$  (Fig. 3(a)) the charge curve increased from 1.03 V to 1.57 V, the discharge curve decreased inversely from 1.57 V to 1.03 V, and they meet at the midpoint of each curve. The energy loss of the battery due to the overvoltage is negligible during both the charging and the discharge processes. On the other hand, in the case of  $k_0 = 10^{-3} \text{ cm s}^{-1}$  (Fig. 3(b)), the charge curve shifts to a higher voltage and the discharge curve shifts to a lower voltage. Since the contribution of the overvoltage cannot be neglected, the battery using the active material with the small  $k_0$  requires more energy in the charged stage but discharges less energy. The charge and the discharge curves of the neptunium battery and the vanadium battery

were evaluated by assuming the same open circuit voltage of 1.30 V as in the Section 2 and the standard rate constants for the neptunium or the vanadium electrode reactions determined at the PFC electrode in this study. The values of the standard rate constants of the positive ( $k_{0,p}$ ) and the negative reactions ( $k_{0,n}$ ) used are  $k_{0,p} = 2.1 \times 10^{-2} \text{ cm s}^{-1}$  and  $k_{0,n} = 1.4 \times 10^{-2} \text{ cm s}^{-1}$  for the standard rate constants of Np(V)/Np(VI) and Np(IV)/Np(III) reactions, respectively, and  $k_{0,p} = 8.5 \times 10^{-4} \text{ cm s}^{-1}$  and  $k_{0,n} = 5.1 \times 10^{-4} \text{ cm s}^{-1}$  for the standard rate constants of V(V)/V(IV) and V(III)/V(II) reactions, respectively. In the evaluated curves for the neptunium battery and the vanadium battery, as shown in Fig. 3(c and d), respectively, it should be noted that the curves (c) for the neptunium battery have the feature close to the curves for  $k_0 = 10^{-1}$  as mentioned above. The energy efficiency corresponding to Fig. 3(a–d) is evaluated to be 99.8%, 87.1%, 99.0% and 82.9%, respectively. Also, the energy efficiency of the neptunium battery for different carbon electrodes was evaluated to be 99.0%, 95.7% and 98.8% for the carbon electrode of PG (*c*-plane), PG (*a*-plane) and GC, respectively, which can be compared to the 99.0% for PFC. These results indicate that the PFC and the PG (*c*-plane) are the best carbon electrodes for the neptunium battery.

It is worth noting that the overvoltage has a close relationship with the current density  $j_0$  according to Eq. (5). Therefore, the charged and discharged energy strongly depend on overvoltage determined by a given combination of the standard rate constant  $k_0$  and the current density  $j_0$ . With regards to various  $k_0$  and  $j_0$  values, the energy efficiency of a charge–discharge unit cycle, defined as the ratio of

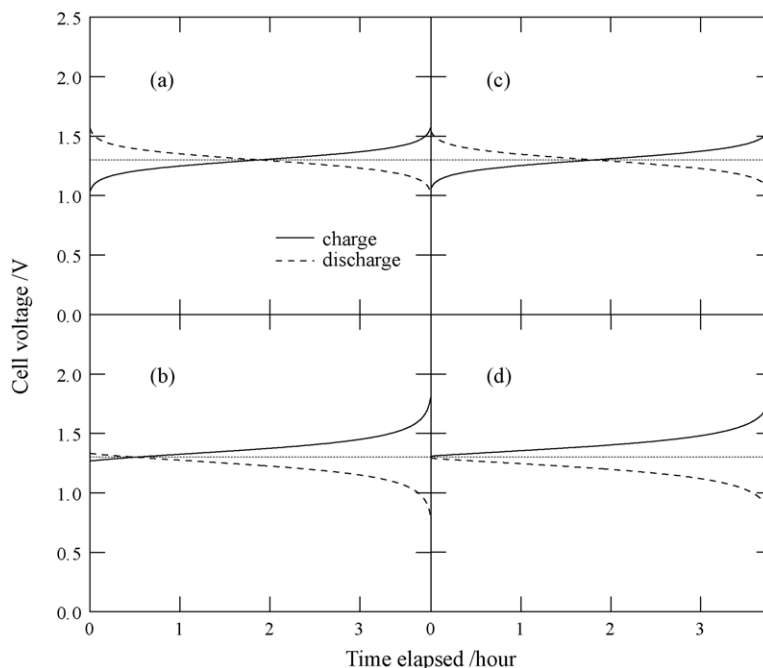


Fig. 3. Charge and discharge curves for current density of  $70 \text{ mA cm}^{-2}$  and the open circuit voltage of 1.30 V with a variety of the standard rate constants for the positive ( $k_{0,p}$ ) and the negative ( $k_{0,n}$ ) electrodes. Values of  $k_{0,p}$  and  $k_{0,n}$  are  $10^{-1}$  and  $10^{-1}$  (a);  $10^{-3}$  and  $10^{-3}$  (b);  $2.1 \times 10^{-2}$  and  $1.4 \times 10^{-2}$  as the neptunium battery (c);  $8.5 \times 10^{-4}$  and  $5.3 \times 10^{-4}$  as the vanadium battery (d).

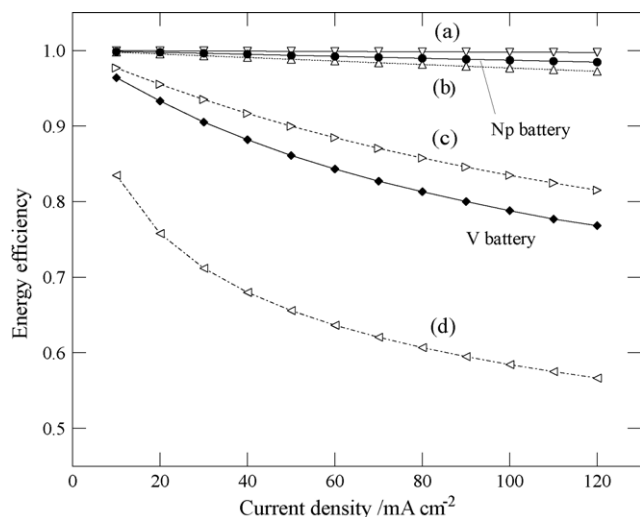


Fig. 4. Energy efficiencies for a charge–discharge unit cycle calculated for a variety of the standard rate constants for the positive ( $k_{0,p}$ ) and the negative ( $k_{0,n}$ ) electrodes and for the neptunium and the vanadium battery assuming the open circuit voltage of 1.30 V. Values of  $k_0 = k_{0,p} = k_{0,n}$  are  $10^{-1} \text{ cm s}^{-1}$  (a),  $10^{-2} \text{ cm s}^{-1}$  (b),  $10^{-3} \text{ cm s}^{-1}$  (c) and  $10^{-4} \text{ cm s}^{-1}$  (d).

the energy required to discharge the battery to the energy required to discharge it,  $E_d/E_c$ , is evaluated by calculating the charge–discharge curves (Fig. 3). As shown in Fig. 3, batteries with active materials with  $k_0 \geq 10^{-2} \text{ cm s}^{-1}$  have very high energy-efficiencies, larger than 97% for  $j_0 \leq 120 \text{ mA cm}^{-2}$ , whereas the energy efficiency decreases dramatically for active materials with  $k_0 < 10^{-2} \text{ cm s}^{-1}$ .

Fig. 4 reveals very clearly the dependence of the energy efficiency on the kinetics of the active materials and the current density of the charging and discharge. For the battery with active materials with  $k_0 > 10^{-2} \text{ cm s}^{-1}$ , the energy efficiency remains almost at unity even when the current density increases to  $100 \text{ mA cm}^{-2}$ . In contrast, for the battery with active materials with  $k_0 < 10^{-3} \text{ cm s}^{-1}$ , the energy efficiency decreases significantly even at low current densities. Comparing the neptunium and the vanadium batteries, for instance, at the current density of  $70 \text{ mA cm}^{-2}$ , which is a typical current density adopted for the existing vanadium battery, the difference in the energy efficiency reaches ca. 16% calculated from the efficiencies of 99.1% and 82.7% for the neptunium and the vanadium batteries, respectively. Therefore, the neptunium battery has an excellent charge and discharge performance as elucidated from the discharge experiment (Fig. 1) and the analysis of the battery (Fig. 4) in comparison with the existing vanadium battery.

## 5. Conclusions

Using the PFC electrode, a non-flow type cell was constructed and the discharge curve was obtained for the neptunium battery with circulation induced by bubbling gas through the electrolyte. We have also obtained the discharge

curve of the vanadium battery. In an alternative to construct the redox-flow cell which is difficult to use the highly radioactive neptunium, a model for evaluating the energy efficiency of the redox-flow battery was developed and we have evaluated the energy efficiency of the neptunium battery as 99.1% at  $70 \text{ mA cm}^{-2}$ , which exceeds that of the vanadium battery by ca. 16%.

## Acknowledgements

We would like to thank Prof. Hajimu Yamana of Kyoto University, Dr. Zenko Yoshida and Dr. Toru Ogawa of Japan Atomic Energy Research Institute, Dr. Ken Nozaki of National Institute of Advanced Industrial Science and Technology for helpful discussion and encouragement. The authors thank the Asahi Kasei Corporation, Japan, for providing ion exchange membranes used in the present study. This work was performed at the Irradiation Experimental Facility, Institute for Materials Research (IMR), Tohoku University, and under the cooperative research program of IMR, Tohoku University. This work is supported by the Nuclear Research Promotion Program (JANP) of the Japan Atomic Energy Research Institute and a Grant-in-Aid for Scientific Research from The Ministry of Education, Culture, Sports, Science and Technology.

## References

- [1] J. Hindman, L. Magnuson, T. Lachapelle, *J. Am. Chem. Soc.* 71 (1949) 687–693.
- [2] Y. Shiokawa, H. Yamana, H. Moriyama, *J. Nucl. Sci. Technol.* 37 (2000) 253–256.
- [3] L.H. Thaller, Electrically rechargeable REDOX flow cell. US Patent 3,996,064 (December 7, 1976).
- [4] T. Yamamura, Y. Shiokawa, H. Yamana, H. Moriyama, *Electrochim. Acta* 48 (2002) 43–50.
- [5] T. Yamamura, Y. Shiokawa, Y. Ikeda, H. Tomiyasu, *J. Nucl. Technol. Sci. Suppl.* 3 (2002) 445–448.
- [6] T. Yamamura, Y. Shiokawa, Y. Nakamura, K. Shirasaki, S.-Y. Kim, *J. Alloys Compd.* 374 (2004) 349–353.
- [7] H.G. Heal, *Nature* 157 (1946) 225–225.
- [8] D.M.H. Kern, E.F. Orlemann, *J. Am. Chem. Soc.* 71 (1949) 2102–2106.
- [9] E. Rona, *J. Am. Chem. Soc.* 72 (1950) 4339–4343.
- [10] F.R. Duke, R.C. Pinkerton, *J. Am. Chem. Soc.* 73 (1951) 2361–2362.
- [11] F. Nelson, K.A. Kraus, *J. Am. Chem. Soc.* 73 (1951) 2157–2161.
- [12] B.J. Masters, L.L. Schwartz, *J. Am. Chem. Soc.* 83 (1961) 2620–2624.
- [13] T.W. Newton, F.B. Baker, *Inorg. Chem.* 4 (1965) 1166–1170.
- [14] B. McDuffie, C.N. Reilley, *Anal. Chem.* 38 (1966) 1881–1887.
- [15] G. Gritzner, J. Selbin, *J. Inorg. Nucl. Chem.* 30 (1968) 1799–1804.
- [16] A. Ekstrom, *Inorg. Chem.* 13 (1974) 2237–2241.
- [17] M. Skyllas-Kazacos, M. Rychcik, R.G. Robins, A.G. Fane, M.A. Green, *J. Electrochem. Soc.* 133 (1986) 1057.
- [18] B. Sun, M. Skyllas-Kazacos, *Electrochim. Acta* 37 (1992) 1253–1260.
- [19] E. Sum, M. Rychcik, M. Skyllas-Kazacos, *J. Power Sources* 15 (1985) 179–190.

- [20] E. Sum, M. Rychcik, M. Skyllas-Kazacos, *J. Power Sources* 16 (1985) 85.
- [21] M.T. McDermott, K.R. Kneten, R.L. McCreery, *J. Electrochem. Soc.* 140 (1993) 2593–2599.
- [22] K.K. Cline, M.T. McDermott, R.L. McCreery, *J. Phys. Chem.* 98 (1994) 5314–5319.
- [23] T. Yamamura, N. Watanabe, T. Yano, Y. Shiokawa, *J. Electrochem. Soc.* 152 (2005) A830–A836.
- [24] K. Hasegawa, A. Kimura, T. Yamamura, Y. Shiokawa, *J. Phys. Chem. Solids* 66 (2005) 593–595.
- [25] J.J. Kats, G.T. Seaborg (Eds.), *The Chemistry of the Actinide Elements*, Methuen & Co. Ltd., London, 1957.